NUMERICAL ANALYSIS OF INFLUENCE OF BRANCH FLOW ON THERMAL MIXING IN A T-JUNCTION PIPING SYSTEM

P. Karthick Selvam, Rudi Kulenovic and Eckart Laurien
Institute of Nuclear Technology and Energy Systems (IKE),
Pfaffenwaldring 31, University of Stuttgart
70569 Stuttgart, Germany
karthick.selvam@ike.uni-stuttgart.de; rudi.kulenovic@ike.uni-stuttgart.de;
eckart.laurien@ike.uni-stuttgart.de

ABSTRACT

Fatigue cracking of pipes due to coolant temperature fluctuations near the structure, commonly known as thermal fatigue, is an important safety related issue during the operation of a Nuclear Power Plant. T-junction piping systems, in particular, are more vulnerable to thermal fatigue cracking due to intense mixing of coolant streams at significant temperature differences (ΔT) causing rapid thermal fluctuations near the wall downstream of T-junction. The paper presents Large Eddy Simulation (LES) analyses of thermal mixing of fluids in a T-junction piping configuration to investigate near wall thermal loading characteristics under increasing flow velocities in the branch pipe. LES calculations, performed using CFD software ANSYS CFX 14.0, are based on T-junction piping at Fluid Structure Interaction (FSI) test facility, University of Stuttgart. Hot and cold coolant streams flow in main and branch pipes, respectively. Temperature difference between the mixing fluids (ΔT) is 117 K. Three LES cases with increasing velocity ratios ($v_r = u_{branch}/u_{main}$) are studied to analyze flow mixing behavior downstream of T-junction. At lower velocity ratio (v_r= 0.76, Case 1), a thermally stratified flow with an oscillating stratification layer is observed downstream along the mixing region. At an increased velocity ratio (v_r= 1.52, Case 2), thermally stratified flow with enhanced fluid mixing is observed along the direction of flow. At highest velocity ratio (v_r= 2.28, Case 3) among investigated cases, coolant streams undergo complete turbulent mixing downstream of T-junction. Near wall temperature fluctuations, an important factor contributing to thermal fatigue, have maximum amplitudes ranging from 5.1 % of ΔT (Case 1) through 9.3 % of ΔT (Case 2) to 9 % of ΔT (Case 3) among analyzed positions in the flow near the wall (5D and 6D, with D being diameter of main pipe). The study also revealed significantly higher amplitude of temperature fluctuations near the wall in the vicinity of T-junction (within distance 1D to 4D). Frequency spectrum analyses show energy of temperature fluctuations mainly contained in the range of 0.1 – 4 Hz.

KEYWORDS
T-Junction piping, Branch velocity, Temperature fluctuations, Frequency spectrum

1. INTRODUCTION

High Cycle Thermal Fatigue (HCTF) problems occur in a Nuclear Power Plant (NPP) due to coolant temperature fluctuations near the wall region, which reduces the working life of piping systems subjected to it. Thermal fatigue damage in piping structure has been reported in several NPPs like (i) Tihange-1 (Belgium) (ii) Tsuruga-2 (Japan) (iii) Tomari-3 (Japan) etc. [1] In a T- junction, two fluids at different temperatures and velocities mix together intensively. This results in thermal fluctuations near the piping wall downstream of T-junction inducing cyclical thermal stresses in the structure. Outside the reactor core, this phenomenon occurs frequently in T-junction piping systems in Residual Heat Removal System

(RHRS). One such accident due to HCTF widely reported in literature is the leakage due to a wall-through crack (180 mm long) detected downstream of T-junction in RHRS at Civaux NPP-I. Analysis performed by Chapuliot et al. (2005) [2] highlighted the origin of this phenomenon as thermal degradation caused by HCTF. Due to limitations of time response, HCTF cannot be properly monitored using common thermocouple instrumentation [3]. As a consequence, Computational Fluid Dynamics (CFD) simulations are frequently performed to analyze flow mixing behavior in any region of interest downstream of T-junction. This gives valuable information about flow mixing behavior and the results could also be compared with measurement data in order to analyze the validity of numerical results. An international blind CFD – validation exercise was performed to test the ability of CFD codes to predict flow parameters affecting HCTF and the results were compared with measurements from the benchmark Vattenfall T-junction experiment [4]. Of all the turbulence modeling methods used in this exercise, LES results showed good agreement with measurement data and is also used in the present study.

Numerical investigations of T-junction mixing of fluids under various inflow conditions using LES are found in literature. LES of two types of mixing tee configurations involving five experiments with different velocity ratios were investigated by Hu and Kazimi (2006) [5]. Westin et al. (2008) [6] performed mixing experiments in a T-junction and compared results between LES and Detached Eddy Simulation (DES), with LES results showing good agreement with experimental data. A study of analyzing the suitability of wall-function method in predicting thermal fluctuations in a T-junction using LES was performed by Jayaraju et al. (2010) [7]. Numerical results obtained using wall-function approach showed good agreement with wall-resolved approach in predicting bulk velocity and temperature field, but root mean square (RMS) components are consistently under-estimated close to the wall boundaries. An assessment of the accuracy of LES method for thermal fatigue predictions in a T-junction was performed by Kuczaj et al. (2010) [8] using Vreman subgrid-scale model. In order to obtain numerical solutions that are in good agreement with measurements, it was suggested that the mesh resolution be able to resolve the Taylor micro-scale length. OECD/NEA conducted the Vattenfall T-junction benchmark exercise (Smith et al. (2011) [1]) to provide relevant experimental data to assess the performance of CFD codes in accurately predicting the temperature and velocity data obtained from measurements. Based on this experiment, Ndombo and Howard (2011) [9] performed numerical analysis of thermal mixing in T-junction using LES and a good agreement is obtained with experimental results. LES was performed with turbulent inlet conditions and was seen to have an effect on near wall flow in terms of temperature fluctuations and temperature-velocity correlation, which are responsible for mechanical stresses imposed on the structure. Numerical studies of thermal mixing were performed by Ayhan and Sökmen (2012) [10], Höhne (2013) [11] based on Vattenfall T-junction experiments to estimate frequency of temperature and velocity fluctuations. A comparison of numerical results between LES and Reynolds Averaged Navier Stokes (RANS) methods showed LES results to be in good agreement with experimental data.
The following section deals with description of experimental setup, followed by a discussion of numerical approach applied in the present study. Results obtained from LES calculations are discussed thereafter, followed by concluding remarks summarizing the results and insights obtained from the study.

2. EXPERIMENTAL SETUP

The Fluid Structure Interaction (FSI) test facility at University of Stuttgart is a horizontal piping system with main and branch pipes intersecting at a sharp edged T-junction. The piping material is austenitic stainless steel (X6 CrNiNb 18-10) with reduced carbon content (in accordance with German Nuclear Safety Standards Commission, KTA 3201.1). It is built with the aim of performing T-junction fluid mixing experiments under realistic temperature conditions present in an operating NPP (see Fig. 1). Deionized water is the working fluid and the maximum pressure and temperature under which experiments shall be performed are about 75 bar and 553 K, respectively. The main and branch pipes have inner diameters of 71.8 mm (D) and 38.9 mm (d). More details about the FSI test facility are described in

Kuschewski et al. (2013) [12]. Cold fluid at room temperature from the branch pipe could be circulated at a maximum velocity of 0.084 m/s, corresponding to Reynolds number (Re_b) in the range of only 3200 – 3700 due to the operational limit of the pump used in FSI test facility. Experimental and numerical studies have shown that this velocity is insufficient to cause complete mixing of fluids downstream of T-junction. Hence numerical investigations are performed to study the behavior of thermal mixing at higher branch flow velocities in FSI test facility.

Table I shows the list of LES cases performed in the present study. Of these, Case 1 is validated with measurement data [13] while Cases 2 and 3 are numerical experiments to understand the nature of flow downstream of T-junction at higher branch velocities. This allows us to compare the difference in flow behavior at increased velocities and other necessary parameters between the validated benchmark study (Case 1) and numerical experiments (Cases 2 and 3).

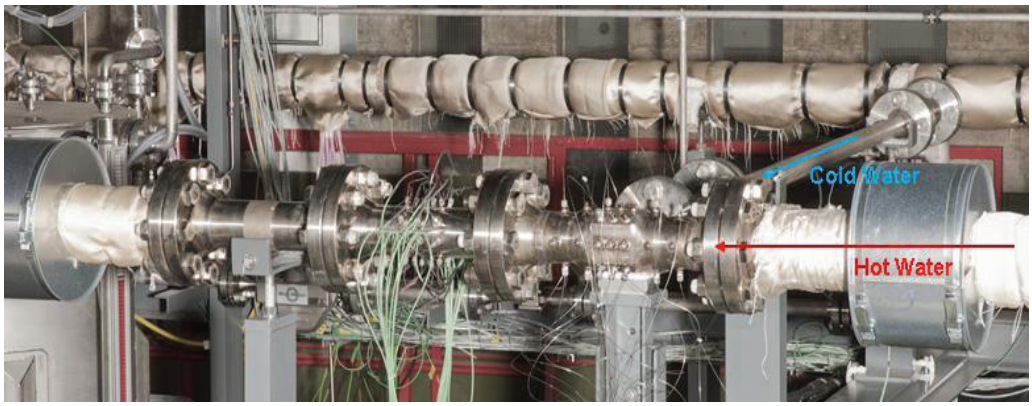

Figure 1. T-junction setup at Fluid Structure Interaction (FSI) test facility

Table I. List of LES cases performed in the study

	u_m* (m/s)	u_b* (m/s)	T_m (K)	T_b (K)	Re_m	Re_b	$V_r = \frac{u_b}{u_m}$
Case 1	0.11	0.08	415	298	36400	3670	0.76
Case 2	0.11	0.17	415	298	36400	7340	1.53
Case 3	0.11	0.25	415	298	36400	11010	2.29

* *Suffixes m and b denotes main and branch pipes respectively*

3. NUMERICAL APPROACH

3.1. Computational Domain

A full scale model of FSI T-junction is used to perform LES and the schematic of computational domain is shown in Fig. 2. Hot fluid flows in main pipe (x-direction) and cold fluid flows in branch pipe (y-direction). Acceleration due to gravity is set along the negative z-direction. The main and branch pipes have lengths of 4D and 5d upstream of T-junction and 20D in the mixing region. LES is performed using ANSYS CFX 14.0, which uses an element based finite volume approach [19]. Monitor points are used in ANSYS CFX to acquire information on any variable of interest at any desired location in the

computational domain. These are placed 2 mm in the flow near the wall region at positions 5D, 6D and 0.15 mm in the structure at 5.5D (experimental thermocouple positions) downstream of T-junction to analyze the effect of increased branch flow (Cases 2 and 3) on mixing conditions and compare them with numerically validated LES data (Case 1). Cross-section of T-junction mesh and angular position of monitor points are shown in Fig. 3.

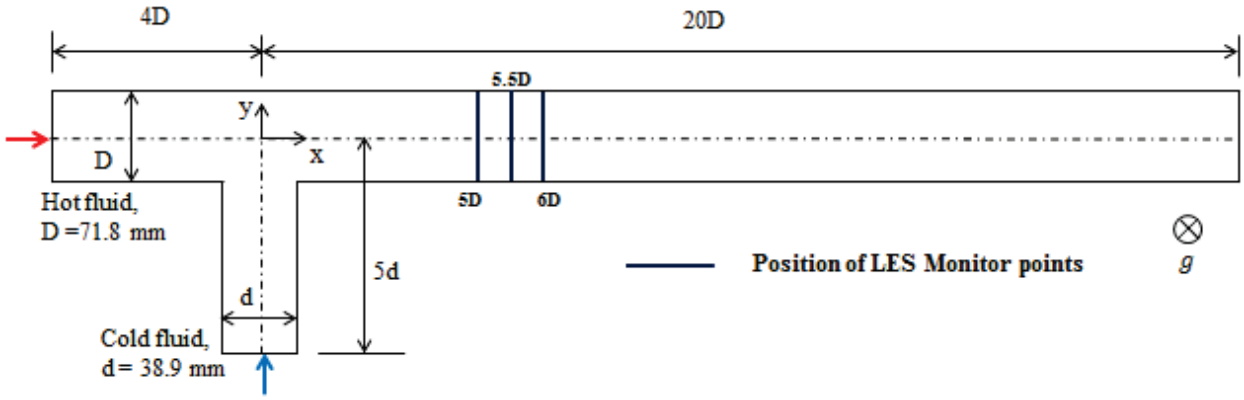

Figure 2. Schematic of T-junction domain used for LES

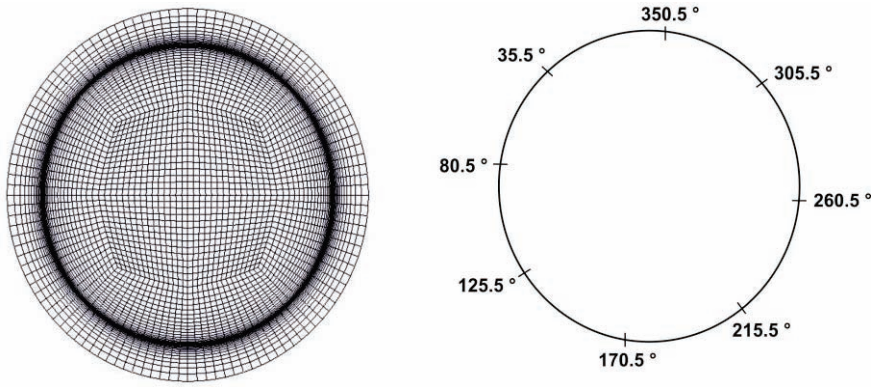

Figure 3. Cross-section of mesh and angular position of monitor points (view towards T-junction)

Three dimensional T-junction grid is constructed using ICEM CFD, a meshing software of ANSYS. It has about 7 million unstructured hexahedral mesh elements. Grid resolution for LES calculations in the present study is chosen on the basis of results obtained from precursor RANS (Reynolds Average Navier Stokes) simulations [14]. This method was seen to give reasonable agreement with measurement data when the mesh is fine enough to resolve Taylor micro-scales in the flow [8]. Two parameters are evaluated thereafter: Taylor micro-scale (λ) and energy length scale (L_R), defined as $\lambda = \sqrt{10k\nu/\varepsilon}$ and $L_R = k^{3/2}/\varepsilon$, respectively. Here k is the turbulent kinetic energy, ε is the turbulent dissipation rate and ν the kinematic viscosity. It was recommended to choose the mesh cell size (Δ) based on the following criterion: $\Delta = \max(\lambda, L_R/10)$. Based on this estimation, the T-junction mesh used in the present study to perform LES has an average cell size of 1.2 mm. This corresponds to a non-dimensional grid spacing in the streamwise (Δx^+), spanwise (Δy^+) and wall-normal (Δz^+) directions [7] of 27 – 49, 16 – 29 and 16 – 29, respectively, for all the investigated cases in the present study.

Fluid temperature fluctuations in the near-wall region are an important factor contributing to thermal fatigue. Hence the computational meshes should be fine enough to resolve small scale motions in this region. In the near-wall region, a non-dimensional parameter called y^+ is used to define boundary layer regions. Viscous stress dominated laminar sublayer is defined as $y^+ < 5$. The buffer layer, a transition region between viscosity dominated and turbulence dominated regions, is defined as $y^+ < 30$. The contribution of viscosity to wall shear stress diminishes beyond $y^+ > 50$ through y = 0.05D [5] [15]. In the present study, the thickness of the first grid near the wall is 0.025 mm, which corresponds to $4 < y^+ < 8$ for all LES cases.

3.2 Large Eddy Simulation (LES)

Large Eddy Simulation represents larger three dimensional unsteady turbulent motions directly, whereas the effects of smaller scale motions are modeled. As stated in Pope (2000) [15], there are four conceptual steps in LES: (i) A filtering operation is performed to decompose the velocity $u\,(x,t)$ into a filtered component $\bar{u}\,(x,t)$ and a residual component $u'\,(x,t)$. The filtered velocity field $\bar{u}\,(x,t)$, which is three dimensional and time dependent, represents the motion of large eddies. (ii) Navier-Stokes equation is used to derive the equations for evolution of filtered velocity field. Applying filtering operation in Navier-Stokes equation results in an additional term known as residual stress tensor (or SGS stress tensor) that arises from residual motions. (iii) Closure is obtained by modeling the residual stress tensor, most simply by an eddy viscosity model. (iv) The filtered equations are solved numerically for $\bar{u}\,(x,t)$, which provides an approximation to the large scale motions in one realization of turbulent flow.
Filtered Navier-Stokes equation [10] is given by

$$\frac{\partial(\rho\bar{u}_i)}{\partial t}+\frac{\partial}{\partial x_j}\left(\rho\bar{u}_i\bar{u}_j\right)= -\frac{\partial\bar{p}}{\partial x_i}+\frac{\partial\sigma_{ij}}{\partial x_j}-\frac{\partial\tau_{ij}}{\partial x_j}+f_i \tag{1}$$

where $\bar{u}$ and $\bar{p}$ represent filtered velocity and pressure. i, j, k are the tensor indices, σ_{ij} is stress tensor due to molecular viscosity, τ_{ij} is the SGS shear stress tensor and f_i is the source term accounting for buoyancy effects in the flow. Eddy viscosity model is used for SGS modeling, which presumes a linear relation between SGS stress tensor and the filtered rate of strain tensor. It is defined as

$$\left(\tau_{ij}-\frac{1}{3}\tau_{kk}\delta_{ij}\right)=-2\mu_t\bar{S}_{ij} \tag{2}$$

where μ_t is eddy viscosity to be modeled. $\bar{S}_{ij}$ is the rate of strain tensor for the resolved scale and is given by

$$\bar{S}_{ij}=\frac{1}{2}\left[\frac{\partial\bar{u}_i}{\partial x_j}+\frac{\partial\bar{u}_j}{\partial x_i}\right] \tag{3}$$

Eddy viscosity is modeled using Wall Adaptive Local Eddy Viscosity (WALE) [16] model and is defined as

$$\mu_t=\rho(C_w\Delta)^2\frac{\left(S_{ij}^d\,S_{ij}^d\right)^{3/2}}{\left(\bar{S}_{ij}\,\bar{S}_{ij}\right)^{5/2}+\left(S_{ij}^d\,S_{ij}^d\right)^{5/4}} \tag{4}$$

C_w is WALE model constant and S_{ij}^d denotes the traceless part of the square of the velocity gradient tensor.

The conservation of energy equation is defined as

$$\frac{\partial(\rho\bar{h})}{\partial t} + \frac{\partial}{\partial x_j}\left(\rho\bar{h}\bar{u}_j\right) = \frac{\partial}{\partial x_j}\left(\lambda_{\text{eff}}\frac{\partial\bar{T}}{\partial x_j}\right) \quad (5)$$

where $\bar{h}$ and $\bar{T}$ represent filtered enthalpy and temperature, λ_{eff} represents an effective coefficient which includes both molecular conduction and SGS contribution and is defined as

$$\lambda_{\text{eff}} = \lambda + \frac{\mu_t c_p}{Pr_t} \quad (6)$$

where λ is thermal conductivity, c_p is specific heat capacity at constant pressure, μ_t is turbulent eddy viscosity and Pr_t is turbulent Prandtl number.

3.2.1. Initial and boundary conditions

- Steady state simulation of T-junction fluid mixing is performed using $k-\omega$ based Shear Stress Transport ($k-\omega$ SST) turbulence model.
- LES cases are initialized using the previously converged solution of steady state simulations.
- From experimental data, it is observed that hot fluid flowing in the main pipe upstream of T-junction is thermally stratified and this phenomenon is implemented at the hot inlet using profile boundary condition option in ANSYS CFX.
- The physical properties of water like density and viscosity vary with temperature. This variation is implemented using the IAPWS library [17] functionality, a default feature in ANSYS CFX.
- Conjugate heat transfer is applied at the fluid solid interface region. Adiabatic heat transfer boundary condition is used at the outer wall region.
- Kuczaj et al. (2008) [18] and Westin et al. (2008) [6] performed numerical studies and observed that the main generation of turbulence is caused by the mixing of fluids and therefore no perturbation of the fluid flow is applied at the inlets.

The physical time step (Δt) for simulations is chosen to keep the Courant number less than unity in each coefficient loop iteration. Based on previous studies and trial calculations, Δt is chosen to be 0.2 ms for all LES cases. The total physical time simulated for Cases 1, 2 and 3 are 20 s, 17 s and 15 s, respectively. Last 6 seconds of LES data in each case, being statistically steady, were used for calculating turbulent statistics.

4. RESULTS

Fluid temperatures are normalized using temperature difference between the mixing fluids (ΔT). Normalized instantaneous, mean and rms (root mean square) temperatures are defined as follows:

Instantaneous temperature (T^*)	Mean temperature ($\overline{T^*}$)	Temperature fluctuation (T^*_{rms})
$T^* = \frac{T - T_b}{T_m - T_b}$ (7)	$\overline{T^*} = \frac{1}{N}\sum_{i=1}^{N} T^*$ (8)	$T^*_{rms} = \sqrt{\frac{1}{N}\sum_{i=1}^{N}(T^* - \overline{T^*})^2}$ (9)

Here N is the number of sampled data points.

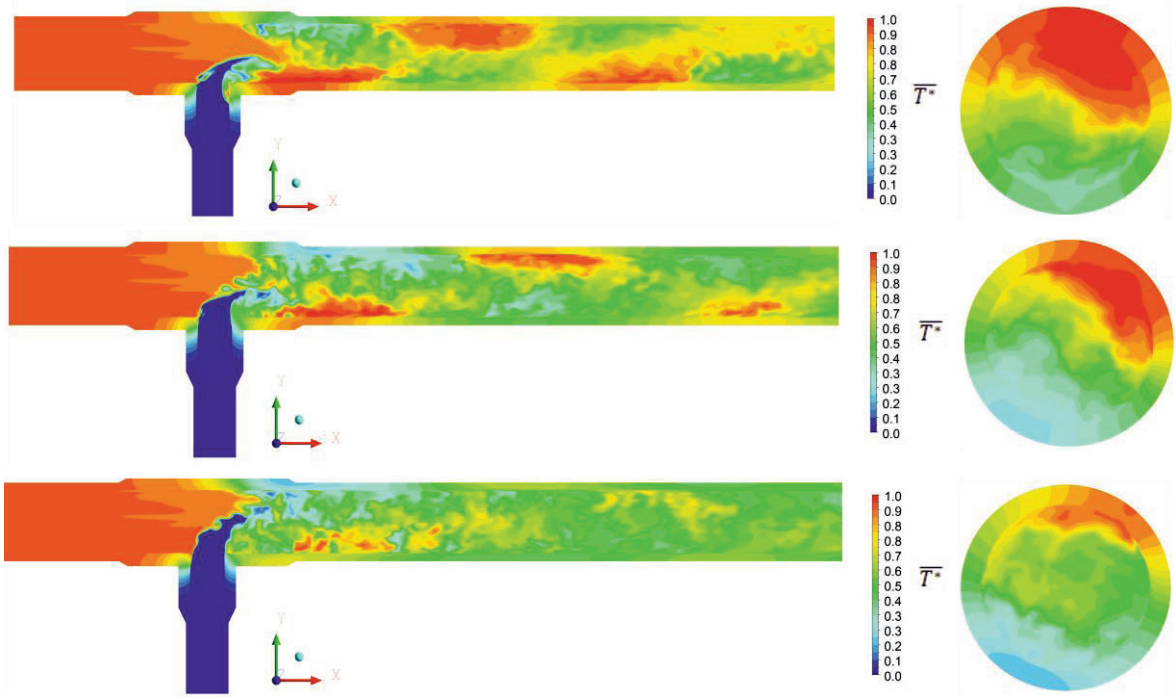

Figure 4. Instantaneous temperature contours along axial (left) and cross-sectional (at x=5D) directions for Case 1 (top, at t = 20 s), Case 2 (middle, at t = 17 s), Case 3 (bottom, at t = 15 s)

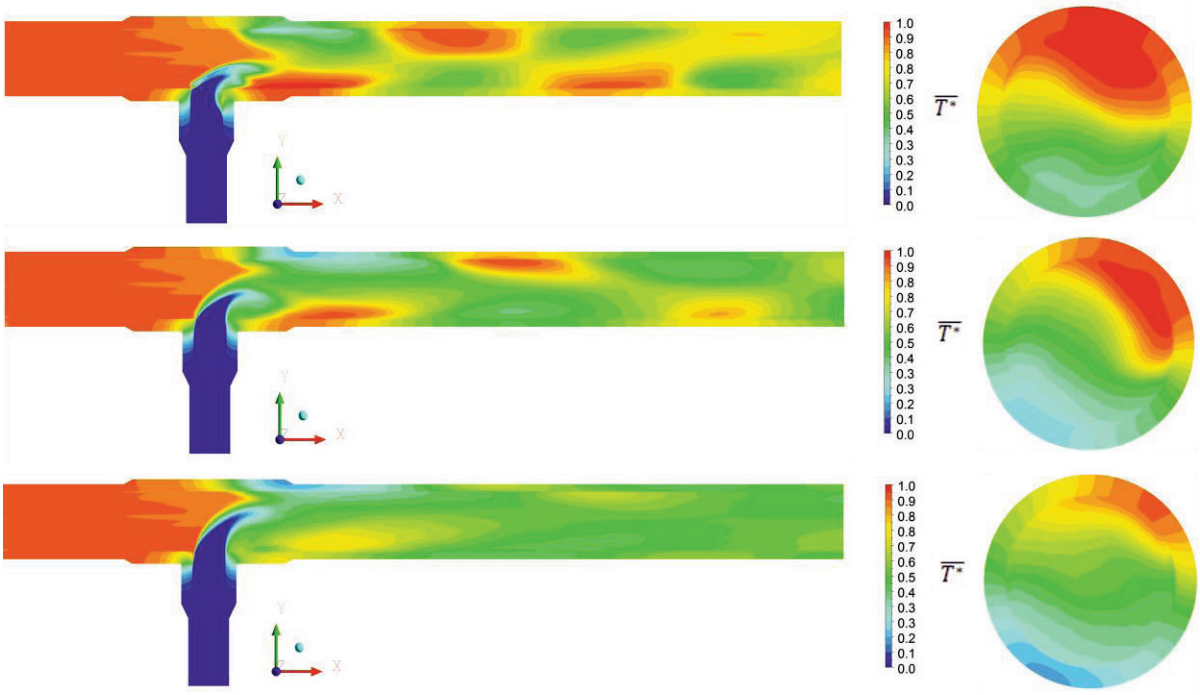

Figure 5. Mean temperature contours along axial (left) and cross-sectional (at x=5D) directions for Case 1 (top), Case 2 (middle), Case 3 (bottom)

4.1 Flow Mixing Behavior

Figs. 4 and 5 show the instantaneous and mean temperature distribution along the axial and cross-sectional planes in the mixing zone downstream of T-junction. The movement of cold fluid towards the opposite wall of main pipe with increase in velocity and its corresponding effect on the mixing behavior is illustrated in these figures. In Case 1, cold fluid from the branch pipe travels close to mid-region of main pipe before starting to mix with hot fluid. This mixing is incomplete resulting in a thermally stratified flow with an oscillating stratification layer in the mixing region, as seen from alternating temperature contours downstream of T-junction.

In Case 2, the branch fluid travels farther than in Case 1 due to its increased velocity resulting in enhanced, albeit incomplete mixing of fluids resulting again in a thermally stratified flow in the downstream region. In Case 3-which has the highest branch velocity among investigated cases-cold fluid from the branch pipe travels till the opposite end of main pipe before mixing completely with hot fluid downstream of T-junction. The mixing between fluids is observed to be significantly intense than in Cases 1 and 2. The appearance of more number of instantaneous flow scales (see Figure 4) close to T-junction highlights the effect of increase in velocity on flow behavior in the mixing region.

Buoyancy effects are significant in Cases 1 and 2 as seen from Richardson number ($Ri = g\Delta\rho D/\rho u_{mix}^2$) values in the mixing region of 2.93 and 1.85, respectively. Richardson number greater than 1 indicates significant buoyancy effects in the flow. Forced convection effects are significant in Case 3 (with Ri = 0.7) due to the highest branch velocity among the investigated cases in the present study.

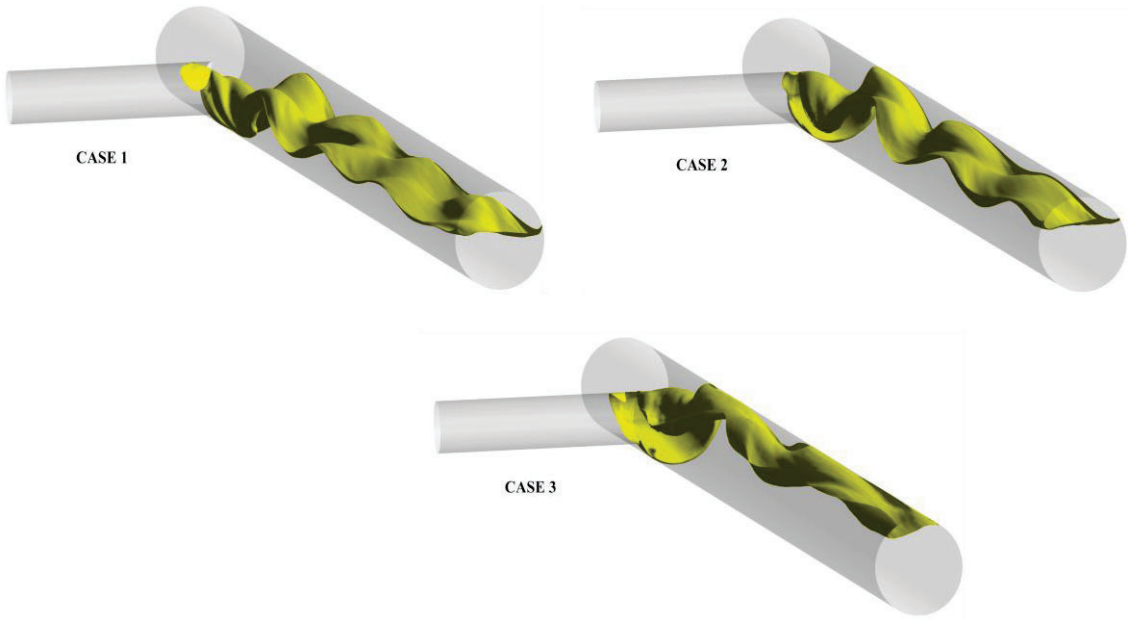

Figure 6. Isosurface of fluid flow for investigated LES cases at mean temperature, $\overline{T^*}$ = 0.75

The nature of fluid flow in the mixing region for all LES cases could also be illustrated using mean temperature isosurfaces shown in Fig. 6. Case 1, with lower branch velocity, exhibits an oscillating wavy flow mixing behavior which attenuates after a certain distance downstream of T-junction. A similar flow behavior at a slightly higher elevation from the bottom of pipe is seen in Case 2, where the oscillating flow behavior is maintained much farther into the mixing region as compared to Case 1. Case 3 does not exhibit the oscillating wavy flow behavior seen in Cases 1 and 2. Fluid from branch pipe falls down in main pipe, then swept to the upper region of the pipe at T-junction and a random flow behavior along downstream region is observed thereafter.

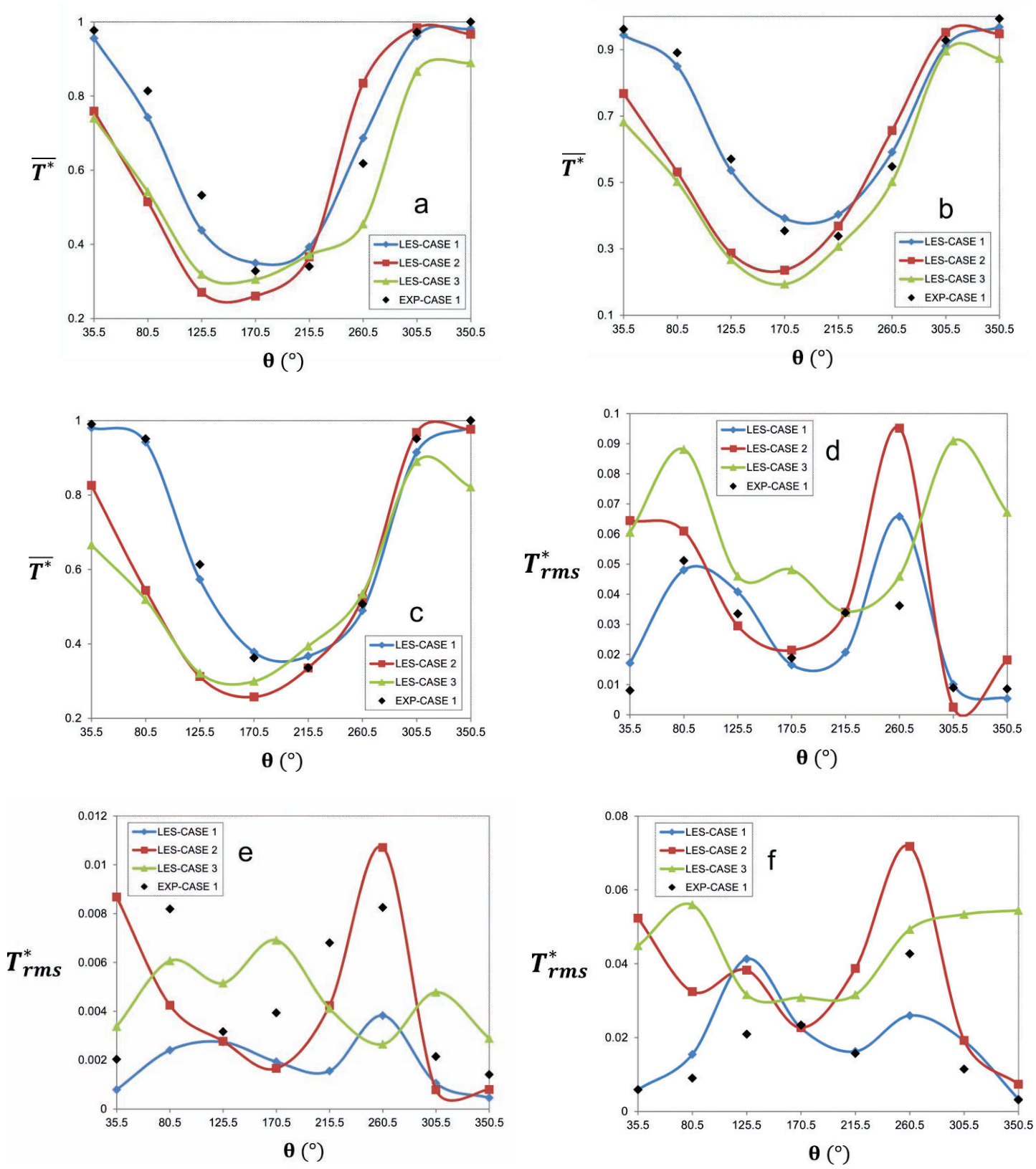

Figure 7. Mean temperature distribution at 5D (a), 5.5D (b) and 6D (c); Distribution of RMS temperature fluctuations at 5D (d), 5.5D (e) and 6D (f)

4.2 Quantitative Assessment of Fluid Mixing

4.2.1 Mean temperature distribution

Fig. 7 (a – c) shows mean temperature ($\overline{T^*}$) distribution near the wall region at positions 5D, 5.5D (in solid) and 6D, respectively. Experimental data from Case 1 is also plotted to compare it with corresponding LES predictions. In Case 1, $\overline{T^*}$ is maximum near the upper cross-sectional pipe region (at θ = 35.5 °, 305.5 ° and 350.5 °) due to buoyancy effects along with relatively lower Reynolds number of the branch fluid. With increase in branch velocity (Cases 2 and 3), $\overline{T^*}$ is reduced by an average 10 – 30 % at angular positions pertaining to upper cross-sectional region. In particular, $\overline{T^*}$ is reduced by about 42 % at 6D (θ = 80.5 ° in Cases 2 and 3) due to increased branch velocity. Lowest $\overline{T^*}$ in each case occurs at angular positions where there is intense mixing of fluids (near lower cross-sectional region at θ = 125.5 °, 170.5 ° or 215.5 °). It is seen that $\overline{T^*}$ values at these angular positions are higher in Case 1 as compared to Cases 2 and 3 indicating the effect of lower branch velocity on less intense flow mixing behavior downstream of T-junction. Mean temperature LES predictions in Case 1 show good agreement with corresponding measurement data.

4.2.2 Distribution of temperature fluctuations

One of the important factors contributing to the risk of HCTF in piping structures are temperature fluctuations near the wall region, which may impose cyclical thermal stresses on piping material resulting in initiation and propagation of fatigue cracks. Fig. 7 (d – f) shows near wall temperature fluctuations (T^*_{rms}) at positions 5D, 5.5D (in solid) and 6D downstream of T-junction. Experimental studies at FSI facility have shown that amplitude of T^*_{rms} is maximum in the vicinity of stratification layer due to significantly higher thermal gradients at this region. A similar observation is seen in LES predictions of cases with thermally stratified flows (Cases 1 and 2). At 5D, maximum T^*_{rms} in all cases have amplitudes in the range of 5 – 10 % of ΔT between the mixing fluids. For Case 1, measurement data indicates T^*_{rms} amplitude to be maximum (about 5.1 % of ΔT) near the stratification layer (at θ = 80.5 °) and this is closely predicted by LES data along with general trend of temperature fluctuation distribution along cross-sectional thermocouple positions. In Case 2, T^*_{rms} amplitude is also predicted to be maximum (about 9.5 % of ΔT) near the stratification layer (at θ = 260.5 °). For Case 3, T^*_{rms} is predicted to be maximum (about 9 % of ΔT) near the upper region (at θ = 305.5 °).

Thermal fluctuations generated in the fluid due to turbulent fluid mixing are significantly attenuated inside the structure, among other reasons, due to thermal inertia of the wall. At position 5.5D, T^*_{rms} amplitude inside the piping structure ranges from 0.04 – 1.2 % of ΔT as flow velocity is increased in branch pipe. Highest T^*_{rms} (0.8 % of ΔT) in Case 1 (from measurement data) is seen to occur near stratification layer (θ = 80.5 ° and 260.5 °). These are highly under-estimated by LES data. At other positions (θ = 35.5 °, 125.5 °, 305.5 ° and 350.5 °), LES predictions in Case 1 show relatively good agreement with measurement data. Highest fluctuation amplitude at position 5.5D in Cases 2 and 3 are predicted to be 1.2 % and 0.6 % of ΔT. At 6D, maximum amplitude of T^*_{rms} is in the range 4.3 – 7.2 % of ΔT between mixing fluids. These are predicted to occur at θ = 260.5 ° (Case 1, about 4.3 % of ΔT), 260.5 ° (Case 2, about 7.2 % of ΔT) and 80.5 ° (Case 3, about 5.6 % of ΔT), respectively. LES predictions of T^*_{rms} in Case 1 closely predict measurement data along most of the angular positions at 6D. Temperature fluctuation amplitude is seen to decrease as the flow proceeds further downstream in mixing region as seen from reduction in T^*_{rms} amplitude at similar angular positions between 5D and 6D.

Another important aspect of the flow is the increase in magnitude of T^*_{rms} at angular positions θ = 305.5 ° and 350.5 ° with increase in branch velocity. There is little mixing of fluids at these positions in Cases 1 and 2 due to thermally stratified flow in mixing region resulting in lower T^*_{rms} amplitude in the range 0.5 – 2 % of ΔT. But in Case 3, T^*_{rms} amplitude is predicted to be 3 – 9 times that of other two cases.

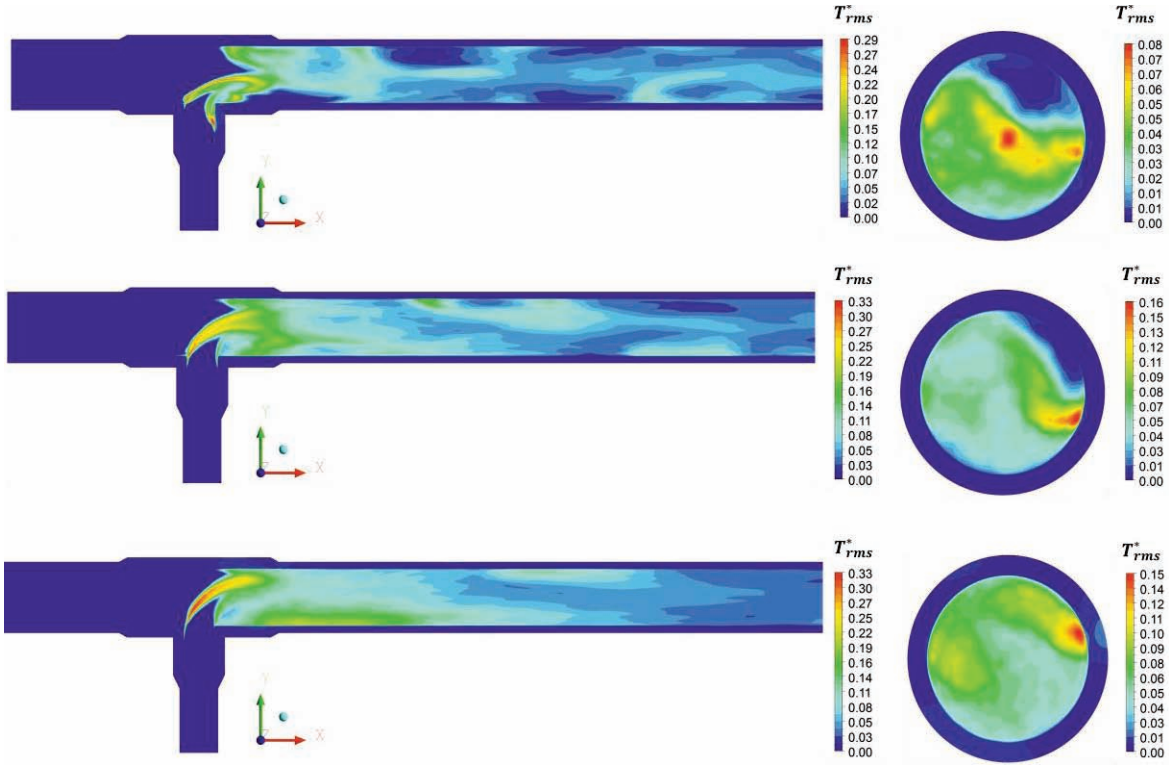

Figure 8. RMS temperature fluctuation contours along axial (left) and cross-sectional (at x=5D) directions for Case 1 (top), Case 2 (middle), Case 3 (bottom)

Fig. 8 shows temperature fluctuations along axial and cross-sectional directions in all LES cases. At T-junction, the mixing interface between hot and cold fluids generate highest T^*_{rms} in all cases, ranging from 29 – 33 % of ΔT (see Fig. 8, left). As described above, highest T^*_{rms} in the near-wall region occurs along the stratification layer in Cases 1 and 2, and the turbulent mixing interface of hot and cold fluid near the upper cross-sectional region in Case 3 (see Fig. 8, right). Another important aspect of the flow behavior under prevailing conditions in the FSI test facility is the occurrence of much higher amplitude temperature fluctuations at other near-wall positions apart from the investigated thermocouple positions as explained in Schuler et al. [22]. It is based on the novel near-wall light emitting diode induced fluorescence technique which showed a positional change of 10 mm could cause a change of T^*_{rms} by a factor of up to 2 or 3.

Apart from the assessment of temperature fluctuations at experimental thermocouple locations, it is also useful to analyze the impact of higher branch velocities close to the top region (as there is nearly very little mixing in Cases 1 and 2). Figure 9 shows the variation of T^*_{rms} along the computational domain at 2 mm in the fluid and 0.15 mm in the solid close to top wall region (at θ = 360 °). No significant fluctuations occur in Case 1 (less than 1 % of ΔT) as seen from negligible T^*_{rms} amplitudes throughout the domain. Case 2 has considerable T^*_{rms} amplitude (maximum T^*_{rms} of 4 % of ΔT at position 5D) near the top wall region for first few diameters downstream of T-junction. Cyclical variation of fluctuations indicates the effect of oscillation of flow along downstream region. A completely different scenario is observed in Case 3, which has maximum T^*_{rms} amplitude of 15.5 % of ΔT (at position 2.6D) indicating the impact of high branch velocity on temperature fluctuation amplitudes following flow mixing at T-junction. A gradual reduction in T^*_{rms} amplitude occurs thereafter. When analyzing temperature fluctuations at other regions, namely, near the side wall and bottom regions, T^*_{rms} amplitudes are seen to be significantly higher (in the range 15 – 25 % of ΔT) for the first few diameters (< 4D) following T-junction in all LES cases as opposed to top region (where Case 3 exhibited significant T^*_{rms} amplitude due to high branch velocity). T^*_{rms} amplitudes in the solid along computational domain is significantly

damped in related to what is observed in the fluid in the near-wall region and Case 3 exhibited highest amplitude (around 1.2 % of ΔT at position 2.5D downstream of T-junction) in the solid among investigated cases at the top wall region.

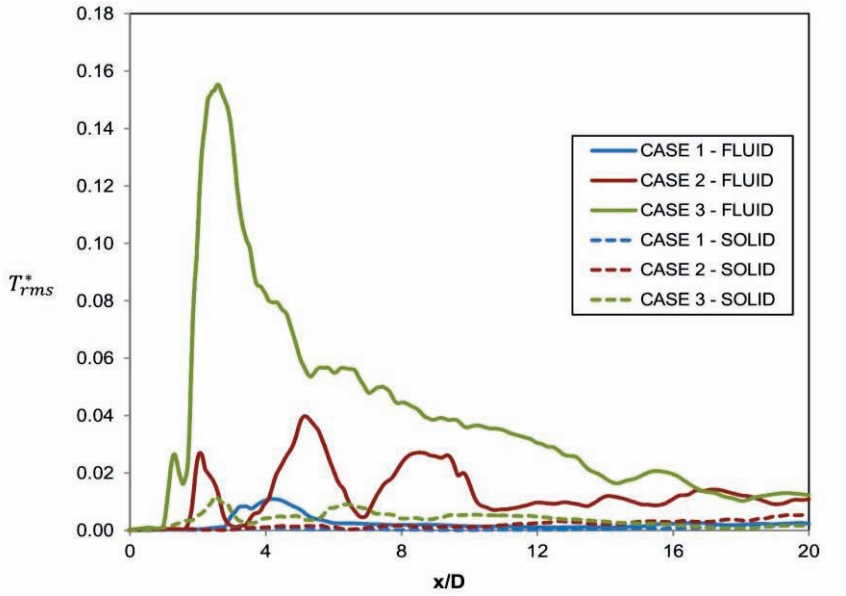

Figure 9. Comparison of T^*_{rms} along flow direction near top wall for all LES cases

4.2.3 Frequency distribution of temperature fluctuations

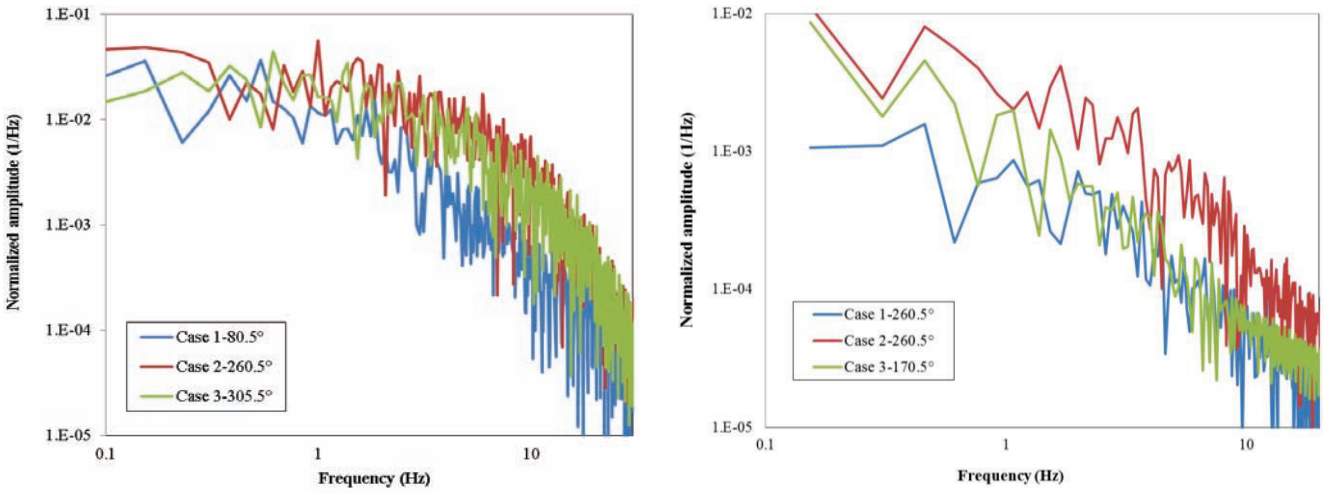

Figure 10. Frequency spectrum of temperature fluctuations in fluid (at 5D, left), solid (at 5.5D, right)

Thermal stresses induced by temperature fluctuations near the pipe wall causes greater damage to piping structure in a certain frequency range enabling propagation of macroscopic cracks. Fluid temperature fluctuations in the high frequency range cannot penetrate the piping structure because of the associated heat transfer loss from fluid to structure, which results in low amplitude thermal stress. On the other hand, very low frequency temperature fluctuations may not cause large thermal stresses due to thermal homogenization in materials [21]. Thermal fatigue analyses performed by Chapuliot et al.(2005) [2]

indicate the range of critical frequencies to be in the range 0.1 – 10 Hz. Therefore, temperature fluctuations in this frequency range are analyzed for all LES cases.

Figure 10 shows frequency spectrum of high amplitude temperature fluctuations in angular positions located in the fluid and solid. The sampling frequency of the signal is 5 kHz and the amplitudes are normalized (using ΔT) in all cases. As a consequence of incomplete mixing of fluids resulting in thermally stratified flows in Cases 1 and 2, high amplitude frequencies occur at angular positions near stratification layer, at either θ = 80.5° or 260.5 °. In Case 3, high amplitude frequencies are predicted to occur near the upper region at θ = 305.5° (at 5D). Also, amplitudes of fluctuations are higher in Cases 2 and 3, due to higher branch velocities, than in Case 1 with lowest branch velocity. Frequency spectrum of temperature fluctuations in the solid (Fig. 10, right) are highly attenuated due to thermal inertia of the steel pipe walls and their amplitudes are seen to be lower by nearly an order of magnitude than the corresponding amplitudes predicted in the flow. Highest amplitude in the solid is observed in Case 2 (at θ = 260.5°) followed by Case 3 (at θ = 170.5°) and Case 1 (at θ = 260.5°). In terms of dominant high amplitude frequencies (spectral peaks), no spectral peaks are found to occur at the investigated locations and the energy of temperature fluctuations are mainly contained in the frequency range 0.1 – 4 Hz.

Significantly higher amplitude of temperature fluctuations or spectral peaks in the aforementioned frequency range could be expected to occur at positions located near the T-junction (in the range 1D – 4D), which is planned to be investigated for the next phase of this study at higher temperature difference (ΔT > 150 K) between mixing fluids and at higher inflow velocities.

5. CONCLUSIONS

LES analyses of flow mixing in a T-junction at increasing flow velocities in branch pipe at room temperature (298 K) and constant main pipe velocity is discussed in this study. Three LES cases are studied with branch pipe Reynolds number of 3670 (Case 1), 7340 (Case 2) and 11010 (Case 3), respectively. Fluid temperature and Reynolds number in the main pipe are 415 K and 36400. The results are summarized as follows:

- Thermally stratified flow is observed for Cases 1 and 2 with oscillation of the mixing region along the direction of flow.
- Intense mixing of fluids is observed in Case 3 and the flow is characterized by extreme oscillations of mixing region due to much higher branch velocity vis-à-vis Cases 1 and 2.
- Temperature fluctuations (T^*_{rms}) having higher amplitudes occur along the stratification layer in Cases 1 and 2 and near the upper region for Case 3. T^*_{rms} has maximum amplitude of 5.1 % of ΔT for Case 1, about 9 % of ΔT for Cases 2 and 3, respectively.
- Temperature fluctuations are seen to attenuate significantly in the structure with maximum amplitudes ranging from 0.04 – 1.2 % of ΔT. Also, fluctuation amplitudes attenuate with distance downstream of T-junction.
- Frequency spectrum analyses of temperature fluctuations do not exhibit distinct spectral peaks at the investigated angular thermocouple positions in 0.1 – 10 Hz range. Amplitudes in both fluid and solid are higher in Cases 2 and 3, where there is an increased branch velocity, as compared to Case 1 with lowest branch velocity among investigated cases. Energy of temperature fluctuations are mainly contained in the frequency range 0.1 – 4 Hz.

ACKNOWLEDGMENTS

The first author would like to thank German Academic Exchange Service (DAAD) Exchange Service (DAAD) for providing research fellowship during the stay at IKE, University of Stuttgart.

REFERENCES

1. "Report of the OECD/NEA-Vattenfall T-Junction Benchmark exercise," https://www.oecd-nea.org/nsd/docs/2011/csni-r2011-5.pdf (2011).
2. S. Chapuliot, C. Gourdin, T. Payen, J.P. Magnaud, A. Monavon, "Hydro-thermal-mechanical analysis of thermal fatigue in a mixing tee," *Nucl. Eng. Des.* **235**, pp. 575 – 596 (2005).
3. C. Walker, M. Simiano, R. Zboray, H.M. Prasser, "Investigations on mixing phenomena in single-phase flow in a T-junction geometry," *Nucl. Eng. Des.* **239**, pp. 116 –126 (2009).
4. B.L. Smith, J.H. Mahaffy, K. Angele, "A CFD benchmarking exercise based on flow mixing in a T-junction," *Nucl. Eng. Des.* **264**, pp. 80 – 88 (2013).
5. L.W. Hu and M.S. Kazimi, "LES benchmark study of high cycle temperature fluctuations caused by thermal striping in a mixing tee," *Int. J. Heat Fluid Flow* **27**, pp. 54 – 64 (2006).
6. J. Westin, C. 't Mannetje, F. Alavyoon, P. Veber, L. Andersson, U. Andersson, J.Eriksson, M. Henriksson, C. Andersson, "High-cycle thermal fatigue in mixing tees. Large-Eddy Simulations compared to a new validation experiment," *Proceedings of 2008 International Conference on Nuclear Engineering (ICONE' 08)*, Orlando, Florida, USA, May 11–15 (2008).
7. S.T. Jayaraju, E.M.J. Komen, E. Baglietto, "Suitability of wall-functions in Large Eddy Simulation for thermal fatigue in a T-junction," *Nucl. Eng. Des.* **240**, pp. 2544 – 2554 (2010).
8. A.K. Kuczaj, E.M.J. Komen, M.S. Loginov, "Large-eddy simulation study of turbulent mixing in a T-junction," *Nucl. Eng. Des.* **240**, pp. 2116 – 2122 (2010).
9. J. Ndombo and R.J.A. Howard, "Large Eddy Simulation and the effect of the turbulent inlet conditions in the mixing Tee," *Nucl. Eng. Des.* **241**, pp. 2172 – 2183 (2011).
10. H. Ayhan, C.N. Sökmen, "CFD modeling of thermal mixing in a T-junction geometry using LES model," *Nucl. Eng. Des.* **253**, pp. 183 – 191 (2012).
11. T. Höhne, "Scale resolved simulations of the OECD/NEA-Vattenfall T-junction benchmark" *Nucl. Eng. Des.* **269**, pp. 149 – 154 (2014).
12. M. Kuschewski, R. Kulenovic, E. Laurien, "Experimental setup for the investigation of fluid-structure interactions in a T-junction," *Nucl. Eng. Des.* **264**, pp. 223 –230 (2013).
13. P. Karthick Selvam, R. Kulenovic, E. Laurien, "Large eddy simulation on thermal mixing of fluids in a T-junction with conjugate heat transfer," *Nucl. Eng. Des.* **284**, pp. 238 – 246 (2015).
14. Y. Addad, U. Gaitonde, D. Laurence, S. Rolfo, "Optimal unstructured meshing for large eddy simulations," *ERCOFTAC Series, Quality and Reliability of Large-Eddy Simulations*, **12**, pp. 93–103 (2008).
15. S.B. Pope, *Turbulent Flows,* pp. 558-561, Cambridge University Press, Cambridge, United Kingdom (2000).
16. F. Nicoud and F. Ducros, "Subgrid-scale modelling based on the square of the velocity gradient tensor," *Flow Turbul. Combust.* **62**, pp. 183 – 200 (1999).
17. W. Wagner and A. Kruse, *Properties of water and steam. The industrial standard IAPWS-IF97 for thermodynamic properties and supplementary equations for other properties*, Springer-Verlag, Berlin, Germany (1998).
18. A.K. Kuczaj, B. de Jager, E. Komen, "An assessment of Large-Eddy Simulation for thermal fatigue prediction," *Proceedings of 2008 International Congress on Advances in Nuclear Power Plants (ICAPP '08)*, Anaheim, California, USA, June 8-12 (2008).
19. ANSYS CFX-Solver Theory Guide (2011).
20. B.A. Kader, "Temperature and Concentration Profiles in Fully Turbulent Boundary Layers," *Int. J. Heat Mass Transfer* **24**, pp. 1541-1544 (1981).
21. N. Kasahara, H. Takasho, A. Yacumpai,"Structural response function approach for evaluation of thermal striping phenomena," *Nucl. Eng. Des.* **212**, pp. 281 – 292 (2002).
22. X. Schuler, E. Laurien, K.-H Herter, S. Moogk, D. Klören, R. Kulenovic, M. Kuschewski, "Thermal fatigue: Fluid-structure interaction at thermal mixing events", 38th MPA Seminar, Stuttgart (2012).